Coherent Heteronuclear Spin Dynamics in an Ultracold Spinor Mixture

Xiaoke Li,[1] Bing Zhu,[1] Xiaodong He,[1] Fudong Wang,[1] Mingyang Guo,[1] Zhi-Fang Xu,[2] Shizhong Zhang,[3] and Dajun Wang[1,*]

[1]*Department of Physics, The Chinese University of Hong Kong, Hong Kong, China*

[2]*Department of Physics and Astronomy, University of Pittsburgh, Pittsburgh, Pennsylvania 15260, USA*

[3]*Department of Physics and Centre of Theoretical and Computational Physics, The University of Hong Kong, Hong Kong, China*

(Received 10 February 2015; revised manuscript received 5 May 2015; published 25 June 2015)

We report the observation of coherent heteronuclear spin dynamics driven by interspecies spin-spin interaction in an ultracold spinor mixture, which manifests as periodical and well-correlated spin oscillations between two atomic species. In particular, we investigate the magnetic field dependence of the oscillations and find a resonance behavior which depends on *both* the linear and quadratic Zeeman effects and the spin-dependent interaction. We also demonstrate a unique knob for controlling the spin dynamics in the spinor mixture with species-dependent vector light shifts.

DOI: 10.1103/PhysRevLett.114.255301 PACS numbers: 67.85.-d, 03.75.Mn, 05.30.Jp, 51.10.+y

Understanding collective spin dynamics is a problem of fundamental importance in modern many-body physics. Central to this understanding is the role of spin-spin interactions and their interplay with the Zeeman energy. In this regard, the ultracold spinor quantum gas [1] provides a powerful platform for investigating spin dynamics due to its high controllability. So far, a rich variety of phenomena have been explored experimentally, including spin oscillations in spinor Bose-Einstein condensate [2–10] and in thermal Bose gases [11], as well as various types of spin textures [12–15]. Very recently, coherent spin oscillations in a spinor Fermi gas [16] and its relaxation [17] have been investigated.

Until now, however, spin dynamics in ultracold atoms has been explored only in a single atomic species. Here, we realize a system consisting of distinguishable spin-1 ^{87}Rb and ^{23}Na atoms, and demonstrate well-controlled and long-lived coherent spin oscillations between them. Our study brings out several unique features of the spinor mixtures. (i) For collisions between two distinguishable spin-1 atoms, the interaction takes place over all three total spin $F = 0, 1$, and 2 channels [18–24], while only $F = 0$ and 2 are allowed for homonuclear collisions. (ii) Unlike the single species case, where only quadratic Zeeman effect is important due to magnetization conservation [25], in spinor mixtures, both linear and quadratic Zeeman effects are important. (iii) The two species have very different vector light shifts, which can be used to generate a differential effective magnetic field. Together with the external magnetic field, this can be used to further control the spin dynamics.

The interaction between two heteronuclear spin-1 bosons at a distance $\mathbf{r}$ can be written as [18,19]

$$V_{12}(\mathbf{r}) = (\alpha + \beta \mathbf{f}_1 \cdot \mathbf{f}_2 + \gamma P_0)\delta(\mathbf{r}), \quad (1)$$

where $\alpha = (g_1 + g_2)/2$ represents the spin-independent interaction. The spin-dependent terms are given by $\beta = (g_2 - g_1)/2$ and $\gamma = (2g_0 - 3g_1 + g_2)/2$, where γ operates only in the $F = 0$ channel via the projection operator P_0. $\mathbf{f}_1$ and $\mathbf{f}_2$ label the hyperfine spins of two different atoms. The coupling constants $g_F = 2\pi\hbar^2 a_F/\mu$ are determined by the s-wave scattering lengths a_F of the corresponding F channels and the reduced mass μ, with $\hbar$ the Planck's constant. From previous studies [26,27], we have determined $(\alpha, \beta, \gamma) = 2\pi\hbar^2 a_B/\mu \times (78.9, -2.5, 0.06)$, where a_B is the Bohr radius. Similar to homonuclear spinor gases of ^{23}Na and ^{87}Rb, both β and γ are much smaller than α [28]. The negative β indicates a ferromagnetic heteronuclear spin-spin interaction, which tends to align the spins of the two species along the same direction.

Let us consider the collision between a ^{87}Rb atom in spin state $|m_1\rangle$ and a ^{23}Na atom in spin state $|m_2\rangle$, which we denote as $|m_1, m_2\rangle$ in the following. Here $m = \pm 1, 0$ are the three Zeeman sublevels of the $f = 1$ hyperfine state. The magnetic energy associated with $|m_1, m_2\rangle$ will be denoted as $E^{m_1,m_2}(B)$. The aforementioned β and γ terms can support several possible heteronuclear spin-changing processes given that the atom numbers of individual species and the system's total magnetization are conserved [36]. This is in stark contrast to the homonuclear spin-1 case, where only one spin-changing process $2|0\rangle \leftrightarrow |1\rangle + |-1\rangle$ is allowed. In this work, we focus on the following heteronuclear spin-changing process,

$$|0, -1\rangle \leftrightarrow |-1, 0\rangle, \quad (2)$$

which is driven solely by the β term [36].

Intuitively, coherent spin dynamics of Eq. (2) can be understood from the interplay between the spin-dependent interaction energy (β term) and the total Zeeman energy

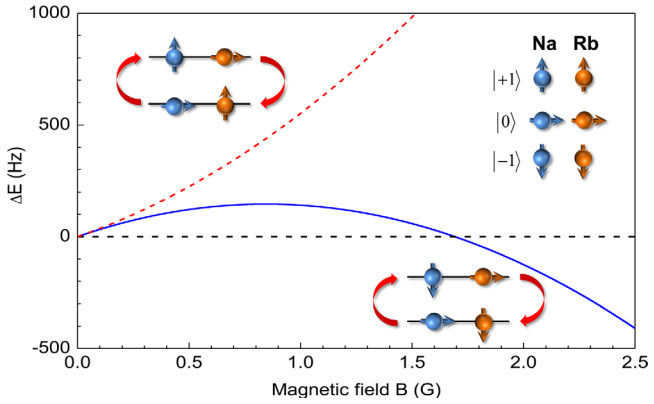

FIG. 1 (color online). Magnetic energy diagram for two heteronuclear spin-changing processes. For the process in Eq. (2) (blue curve), ΔE has a zero-crossing point at $B_0 = 1.69$ G. Spin-changing process $|0,1\rangle \leftrightarrow |1,0\rangle$ (red dashed curve) has a large detuning near B_0 and is greatly suppressed.

difference between these two states: $\Delta E(B) \equiv E^{0,-1}(B) - E^{-1,0}(B)$, as depicted in Fig. 1. In analogy to a driven two-level system, when the two energies are very different, the system undergoes fast but small amplitude detuned oscillations, while when they are comparable, the system oscillates slowly with large amplitude [25]. Since β is small, typical spin-dependent mean-field energy is of the order of 10 Hz, and as a result, visible heteronuclear spin oscillations can only occur near $\Delta E = 0$. As shown in Fig. 1, ΔE depends on the magnetic field B in a non-monotonic manner, and, in particular, vanishes at $B_0 = 1.69$ G, where one expects resonant spin dynamics. This coincidence is a result of the slightly different Landé g factors for ^{23}Na and ^{87}Rb, including contributions from both the linear and the quadratic Zeeman energies [28]. Near B_0, homonuclear spin dynamics is greatly suppressed due to large quadratic Zeeman shifts and other heteronuclear spin-changing processes are also suppressed due to large detuning. For example, the spin-changing process $|0,1\rangle \leftrightarrow |1,0\rangle$ has a magnetic energy difference larger than 1000 Hz and will be substantially suppressed. Thus, working near B_0, we can single out the process in Eq. (2) and obtain clear signatures of heteronuclear spin dynamics.

The considerations above offer only a qualitative picture of the interspecies spin dynamics. Experimentally, we use a bulk sample consisting of an essentially pure ^{23}Na Bose-Einstein condensate and a thermal gas of ^{87}Rb to increase the overlap of the two clouds. This many-body system is distinctively different from the conventional two-level system since spin- and density-dependent mean-field interactions enter nonlinearly into the equations of motion and furthermore, vary in the course of spin dynamics [28]. One important consequence of the many-body effect is the appearance of two magnetically tuned resonances as we shall discuss momentarily.

We produce the ultracold mixture of ^{23}Na and ^{87}Rb atoms in a crossed optical dipole trap (ODT) with both atoms initially prepared in the spin state $|-1\rangle$ [26,37]. To initiate the spin oscillations, we apply a radio-frequency Rabi pulse to simultaneously prepare both Rb and Na in coherent superposition states with most population in the $|-1\rangle$ and $|0\rangle$ states, while population in the $|+1\rangle$ states are typically less than 10%. To monitor the spin dynamics, we detect the fractional spin population $\rho_m^i = N_m^i/N^i$ for each species from the absorption images after various holding time. Here, N_m^i is the atom number of species i in spin state $|m\rangle$. $N^i = N_{-1}^i + N_0^i + N_{+1}^i$ is the total number of atoms of species i, with $i = \mathrm{Na}, \mathrm{Rb}$.

Figures 2(a) and 2(b) show typical time evolution of ρ_m^{Rb} and ρ_m^{Na} at $B = 1.9$ G, respectively. The population in states $|-1\rangle$ and $|0\rangle$ oscillates periodically, while those in state $|1\rangle$ stay nearly constant. It is important to note the following features: (i) States $|-1\rangle$ and $|0\rangle$ of each individual species oscillate with π-phase shift due to number conservation; (ii) the synchronized oscillation between the two species reflects the coherent spin dynamics driven by heteronuclear spin-changing interaction. This is even more clearly exhibited in the individual magnetization dynamics. The fractional magnetization for each species is $\mathcal{M}^i = (N_{+1}^i - N_{-1}^i)/N^i$. The total magnetization of the system is defined as $\mathcal{M} = (N_{+1}^{Na} - N_{-1}^{Na} + N_{+1}^{Rb} - N_{-1}^{Rb})/N$, where $N = \sum_i N^i$ is the total number of atoms. As shown in Figs. 2(c), 2(d) and the inset, $\mathcal{M}^{\mathrm{Na}}$ and $\mathcal{M}^{\mathrm{Rb}}$ are not conserved, but $\mathcal{M}$ is conserved within a few percent. The small variation in $\mathcal{M}$ is comparable to the uncertainties (~5%) in atom number detection. The coherent oscillations of $\mathcal{M}^{\mathrm{Na}}$ and $\mathcal{M}^{\mathrm{Rb}}$ with a π-phase difference is a clear signature of the coherent heteronuclear spin-changing process. The clean oscillations between the $|-1\rangle$ and $|0\rangle$ states also indicate that homonuclear and other heteronuclear spin-changing processes are greatly suppressed.

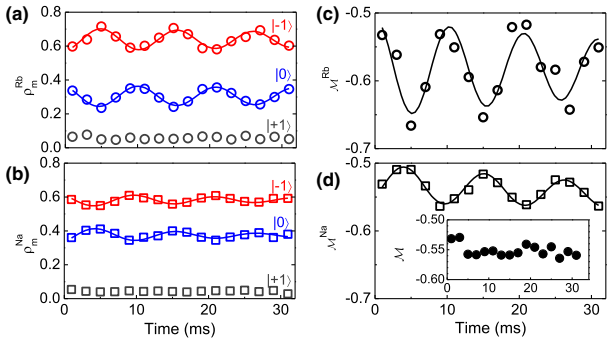

FIG. 2 (color online). Coherent heteronuclear spin dynamics at $B = 1.9$ G. (a),(b), evolution of the fractional spin population of Rb (circle) and Na (square). (c),(d), magnetization oscillations of Rb and Na. The oscillation amplitudes differences are due to the number imbalance. Inset: evolution of total magnetization. Solid lines are sinusoidal fitting.

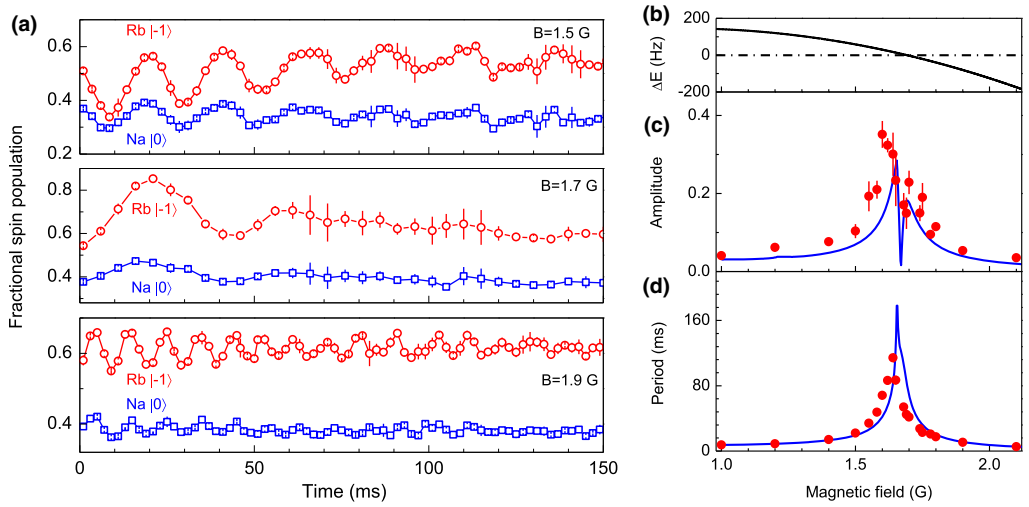

FIG. 3 (color online). Dependence of heteronuclear spin dynamics on external magnetic field B. (a) Spin oscillations at $B = 1.5$ (top), 1.7 (middle), and 1.9 G (bottom) for $|-1\rangle$ of Rb (red circle) and $|0\rangle$ of Na (blue squares). The solid curves are for eye guiding and error bars are from statistics of several shots. (b) Magnetic energy ΔE vs B. (c),(d) Spin oscillation amplitudes (c) and periods (d) extracted from the Rb data. Solid blue lines are calculations based on many-body kinetic equations using experimental atomic conditions without fitting parameters. Error bars for both the amplitude and the period are from fitting of the oscillations and represent 1 standard deviation. Mechanisms for the observed damping in the oscillations will be investigated in future works.

Similar measurements are performed for a range of magnetic fields. Three examples are plotted in Fig. 3(a). Away from B_0, fast oscillation with small amplitude can be observed, while very close to B_0, e.g., at $B = 1.7$ G (middle), the oscillation is slow but with large amplitude. Comparing oscillations at $B = 1.5$ (top) and 1.9 G (bottom), we note that the initial slopes of population change for the same spin states have opposite signs on different sides of B_0. For instance, at the very beginning, the Rb $|-1\rangle$ population decreases at 1.5 but increases at 1.9 G. The same behavior is observed for Na. This is a direct reflection of the sign change of ΔE across B_0, as depicted in Fig. 3(b). These behaviors are well reproduced in our numerical simulations and the initial oscillation directions are consistent with the ferromagnetic spin-changing interaction $\beta < 0$.

We extract the oscillation amplitudes and periods for different magnetic fields and summarize the results in Figs. 3(c) and 3(d). Near B_0, the system is in the interaction dominated regime where an asymmetric double peak appears in the oscillation amplitude with a nonzero dip in between. This can be understood by noting that resonance appears when $|\Delta E|$ and spin-dependent interaction are comparable, which can occur on either side of B_0, analogous to the single species case where the quadratic Zeeman shift is tuned by microwave [38]. However, the exact resonance positions depend also on homonuclear spin-dependent interactions and initial conditions. The double peak is, however, not readily distinguishable in the period where only one peak is observed [28].

To understand the observed spin dynamics quantitatively, we model the Na condensate with the time-dependent Gross-Pitaevskii equation [20,36] and the thermal Rb cloud with the kinetic equation for the Wigner distribution function [39,40]. The dynamics of the two species are coupled through the interaction in Eq. (1). Within the random phase and single mode approximations [28], our simulation agrees quite well with the measurements, as shown in Figs. 3(c) and 3(d). The simulated oscillation period shows only a small kink near B_0, consistent with our experiment conditions. This kink can be regarded as a remnant of the double peak structure that occurs if the numbers of the two species are equal. As the number imbalance increases, one of the peaks gradually disappears, leading to a kink structure in our simulation [28].

A unique feature of the heteronuclear spin dynamics is its dependence on the vector light shift, which is spin and species dependent [28]. In the following, we tune the ellipticity of the ODT beams to further control the spin dynamics. For large detuning Δ exceeding the excited state fine structure splitting Δ_{FS}, the spin-dependent vector light shift is [41]

$$U_m(\vec{r}) \propto \frac{\wp m}{\omega_0^3}\frac{\Delta_{\mathrm{FS}}}{\Delta^2} I(\vec{r}), \tag{3}$$

where ω_0 is the energy splitting between the ground state and the center of the D lines, and $I(\vec{r})$ is the light intensity. The factor $\wp$ characterizes the amount of circular polarization with $\wp = 0$ for linear and $\wp = \pm 1$ for pure $\sigma^{\pm}$ circular polarizations, respectively. U_m can be treated as a "fictitious magnetic field" in the light propagation direction [42]. Its projection, B_{ac}, along the quantization axis alters the effective magnetic field seen by the atoms. Because of

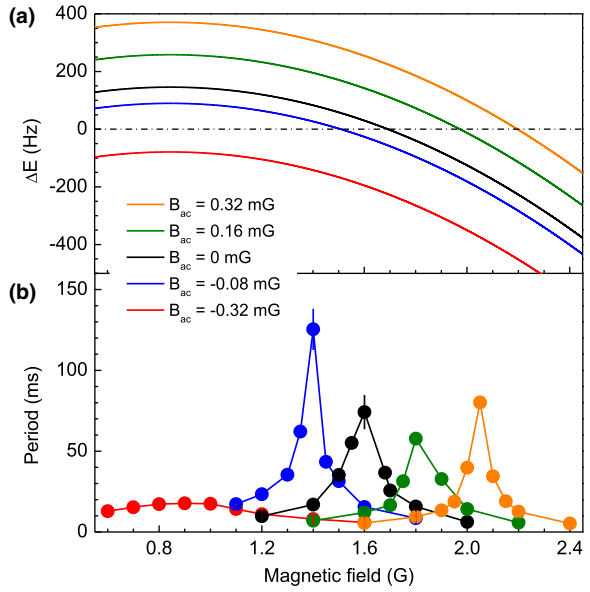

FIG. 4 (color online). Optical control of coherent heteronuclear spin dynamics with vector light shift. (a) Modified dependence of ΔE on B with light induced effective magnetic field B_{ac} on Rb. (b) Resonance positions as observed in the period vary with changing B_{ac}. Solid curves are to guide the eye and error bars are from fitting of the oscillations. B_{ac} is calculated based on the measured light intensity I and $\wp$.

the larger Δ, ω_0 and smaller Δ_{FS} for ^{23}Na, B_{ac} for ^{23}Na is less than 1% of ^{87}Rb. For our final ODT, $B_{ac} \approx 1.6$ mG for Rb and 14 μG for Na if $\wp = 1$. So effectively speaking, by tuning $\wp$, we can control the linear Zeeman energy for Rb and Na independently [28]. The measurements shown in Fig. 2 and Fig. 3 are performed with B_{ac} essentially zero.

Although small, B_{ac} has a dramatic influence on the heteronuclear spin dynamics. For simplicity, we neglect the much smaller B_{ac} for Na. The B_{ac} for ^{87}Rb can shift ΔE significantly, as illustrated in Fig. 4(a). For $B_{ac} < 0$, the zero crossing point is shifted to smaller external magnetic fields. Eventually, for $B_{ac} < -0.2$ mG the entire ΔE curve is shifted to below zero and the zero crossing disappears. In such cases, the spin dynamics will be essentially driven by Zeeman energies with a peak at the field of minimum $|\Delta E|$. When $B_{ac} > 0$, the zero crossing point and thus the resonance position always shifts to higher magnetic field.

Experimentally, $\wp$, and hence B_{ac}, can be tuned by applying the external magnetic field in the horizontal plane and inserting a $\lambda/4$ wave plate into one of the ODT beams. Here $\wp = \sin(2\theta)$, where θ is the angle between the wave plate's axis and the input linear polarization of the light. For the typical θ values in our experiment without causing significant heating, B_{ac} ranges from -0.32 to 0.32 mG. As shown in Fig. 4(b), a rather small B_{ac} can cause a significant change. For example, at $B_{ac} = 0.32$ mG, the resonance is shifted upwards by about 0.4 G. While for negative B_{ac} such that the zero crossing disappears, for example, at $B_{ac} = -0.32$ mG, the line shape of the oscillation becomes much broader, which is a direct manifestation of the oscillation's far off resonance character.

In conclusion, we have observed interaction driven coherent spin-changing dynamics between two different spin-1 Bose gases. Both the oscillation period and amplitude can be tuned over a large range with either external magnetic fields or, quite unique to our system, the species-dependent vector light shift. This latter capability is especially promising because it allows sensitive and versatile control of the spin dynamics, as demonstrated in our experiment.

Our system can serve as an ideal platform for simulating complicated spin systems, such as the coupled electronic and nuclear spin system. Using implementations similar to the two-orbital magnetism model originally proposed for alkali-earth atoms [43], but replacing the two orbits with two different kinds of atoms, the bosonic Kondo model [44,45] may be realized. In addition, in analogy to the generation of entanglement with spin-changing interactions in single species spinor condensates [46,47], the interspecies spin-changing interaction can also be used to generate entanglement between distinguishable atoms [48]. Finally, similar dynamics should exist in other ultracold spinor mixtures. In fact, a proposal for realizing the spontaneous quantum Hall effect and a chiral superfluid with the Bose-Fermi spinor mixture was made recently [49].

We thank Bo Gao for the scattering lengths calculation, Li You, Qi Zhou, Hui Zhai, and Ana Maria Rey for stimulating discussions, and C. K. Law for reading the manuscript. This work is supported by Hong Kong Research Grants Council (General Research Fund Projects CUHK 403813 and CUHK 14305214). Z. F. X. is supported by AFOSR and ARO. S. Z. Z. is supported by Hong Kong Research Grants Council (General Research Fund, HKU 709313P, HKU 17306414 and Collaborative research fund, HKUST3/CRF/13G).

*djwang@phy.cuhk.edu.hk

[1] Y. Kawaguchi and M. Ueda, Phys. Rep. **520**, 253 (2012); D. M. Stamper-Kurn and M. Ueda, Rev. Mod. Phys. **85**, 1191 (2013).
[2] T. Kuwamoto, K. Araki, T. Eno, and T. Hirano, Phys. Rev. A **69**, 063604 (2004).
[3] H. Schmaljohann, M. Erhard, J. Kronjäger, M. Kottke, S. van Staa, L. Cacciapuoti, J. J. Arlt, K. Bongs, and K. Sengstock, Phys. Rev. Lett. **92**, 040402 (2004).
[4] M.-S. Chang, C. D. Hamley, M. D. Barrett, J. A. Sauer, K. M. Fortier, W. Zhang, L. You, and M. S. Chapman, Phys. Rev. Lett. **92**, 140403 (2004).
[5] M.-S. Chang, Q. S. Qin, W. X. Zhang, L. You, and M. S. Chapman, Nat. Phys. **1**, 111 (2005).
[6] A. Widera, F. Gerbier, S. Fölling, T. Gericke, O. Mandel, and I. Bloch, Phys. Rev. Lett. **95**, 190405 (2005).

[7] J. Kronjäger, C. Becker, P. Navez, K. Bongs, and K. Sengstock, Phys. Rev. Lett. **97**, 110404 (2006).
[8] F. Gerbier, A. Widera, S. Fölling, O. Mandel, and I. Bloch, Phys. Rev. A **73**, 041602 (2006).
[9] A. T. Black, E. Gomez, L. D. Turner, S. Jung, and P. D. Lett, Phys. Rev. Lett. **99**, 070403 (2007).
[10] C. Klempt, O. Topic, G. Gebreyesus, M. Scherer, T. Henninger, P. Hyllus, W. Ertmer, L. Santos, and J. J. Arlt, Phys. Rev. Lett. **103**, 195302 (2009).
[11] H. K. Pechkis, J. P. Wrubel, A. Schwettmann, P. F. Griffin, R. Barnett, E. Tiesinga, and P. D. Lett, Phys. Rev. Lett. **111**, 025301 (2013); X. He, B. Zhu, X. Li, F. Wang, Z-F. Xu, and D. Wang, Phys. Rev. A **91**, 033635 (2015).
[12] L. E. Sadler, J. M. Higbie, S. R. Leslie, M. Vengalattore, and D. M. Stamper-Kurn, Nature (London) **443**, 312 (2006).
[13] L. S. Leslie, A. Hansen, K. C. Wright, B. M. Deutsch, and N. P. Bigelow, Phys. Rev. Lett. **103**, 250401 (2009).
[14] J. Y. Choi, W. J. Kwon, and Y. I. Shin, Phys. Rev. Lett. **108**, 035301 (2012).
[15] Y. Eto, H. Saito, and T. Hirano, Phys. Rev. Lett. **112**, 185301 (2014).
[16] J. S. Krauser, J. Heinze, N. Fläschner, S. Götze, O. Jürgensen, D-S. Lühmann, C. Becker, and K. Sengstock, Nat. Phys. **8**, 813 (2012); J. S. Krauser, U. Ebling, N. Flaschner, J. Heinze, K. Sengstock, M. Lewenstein, A. Eckardt, and C. Becker, Science **343**, 157 (2014).
[17] U. Ebling, J. S. Krauser, N. Fläschner, K. Sengstock, C. Becker, M. Lewenstein, and A. Eckardt *et al.*, Phys. Rev. X **4**, 021011 (2014).
[18] T.-L. Ho, Phys. Rev. Lett. **81**, 742 (1998).
[19] T. Ohmi and K. Machida, J. Phys. Soc. Jpn. **67**, 1822 (1998).
[20] C. K. Law, H. Pu, and N. P. Bigelow, Phys. Rev. Lett. **81**, 5257 (1998).
[21] M. Luo, Z. Li, and C. Bao, Phys. Rev. A **75**, 043609 (2007).
[22] Z. F. Xu, Y. B. Zhang, and L. You, Phys. Rev. A **79**, 023613 (2009).
[23] Z. F. Xu, J. Zhang, Y. B. Zhang, and L. You, Phys. Rev. A **81**, 033603 (2010).
[24] Y. Shi, Phys. Rev. A **82**, 023603 (2010).
[25] W. X. Zhang, D. L. Zhou, M. S. Chang, M. S. Chapman, and L. You, Phys. Rev. A **72**, 013602 (2005).
[26] F. D. Wang, D. Z. Xiong, X. K. Li, D. J. Wang, and E. Tiemann, Phys. Rev. A **87**, 050702 (2013).
[27] Bo Gao (private communication).
[28] See Supplemental Material at http://link.aps.org/supplemental/10.1103/PhysRevLett.114.255301 for description of the experimental parameters and procedures, and calculation of the effective magnetic fields induced by vector light shifts. Theoretical calculations are discussed in detail for both two and many-body systems, which includes Refs. [29–35].
[29] G. Reinaudi, T. Lahaye, Z. Wang, and D. Guéry-Odelin, Opt. Lett. **32**, 3143 (2007).
[30] W. J. Kwon, J. Choi, and Y. Shin, J. Korean Phys. Soc. **61**, 1970 (2012).
[31] E. Arimondo, M. Inguscio, and P. Violino, Rev. Mod. Phys. **49**, 31 (1977).
[32] N. N. Klausen, J. L. Bohn, and C. H. Greene, Phys. Rev. A **64**, 053602 (2001).
[33] A. Crubellier, O. Dulieu, F. Masnou-Seeuws, M. Elbs, H. Knöckel, and E. Tiemann, Eur. Phys. J. D **6**, 211 (1999).
[34] A. Widera, F. Gerbier, S. Fölling, T. Gericke, O. Mandel, and I. Bloch, New J. Phys. **8**, 152 (2006).
[35] J. Stenger, S. Inouye, D. M. Stamper-Kurn, H.-J. Miesner, A. P. Chikkatur, and W. Ketterle, Nature (London) **396**, 345 (1998).
[36] Z. F. Xu, D. J. Wang, and L. You, Phys. Rev. A **86**, 013632 (2012).
[37] D. Z. Xiong, X. K. Li, F. D. Wang, and D. J. Wang, arXiv:1305.7091.
[38] L. Zhao, J. Jiang, T. Tang, M. Webb, and Y. Liu, Phys. Rev. A **89**, 023608 (2014).
[39] Y. Endo and T. Nikuni, J. Low Temp. Phys. **152**, 21 (2008).
[40] S. S. Natu and E. J. Mueller, Phys. Rev. A **81**, 053617 (2010).
[41] R. Grimm, M. Weidemüller, and Y. B. Ovchinnikov, Adv. At. Mol. Opt. Phys. **42**, 95 (2000).
[42] C. Cohen-Tannoudji and J. Dupont-Roc, Phys. Rev. A **5**, 968 (1972).
[43] A. V. Gorshkov, M. Hermele, V. Gurarie, C. Xu, P. S. Julienne, J. Ye, P. Zoller, E. Demler, M. D. Lukin, and A. M. Rey, Nat. Phys., **6**, 289 (2010).
[44] L.-M. Duan, Europhys. Lett. **67**, 721 (2004).
[45] M. Foss-Feig and A. M. Rey, Phys. Rev. A **84**, 053619 (2011).
[46] H. Pu and P. Meystre, Phys. Rev. Lett. **85**, 3987 (2000).
[47] L.-M. Duan, A. Sørensen, J. I. Cirac, and P. Zoller, Phys. Rev. Lett. **85**, 3991 (2000).
[48] Y. Shi and Q. Niu, Phys. Rev. Lett. **96**, 140401 (2006).
[49] Z. F. Xu, X. Li, P. Zoller, and W. V. Liu, Phys. Rev. Lett. **114**, 125303 (2015).